Hongwei Gao ✉
Qinhong Fan
Zhibing Chu

https://doi.org/10.21278/TOF.463043422
ISSN 1333-1124
eISSN 1849-1391

SIMULATION RESEARCH ON THE FORMING PROCESS OF LARGE AXLES ROLLED BY CROSS-WEDGE ROLLING

Summary

As a novel metal forming process, cross-wedge rolling (CWR) is widely used in the manufacture of large axles in the rail transportation industry. When the forming process of the axle is studied, its formability becomes one of the key issues in the metal forming process. This paper takes LZ50 axle steel as the research object. Through the application of ANSYS finite element simulation software, combined with previous research and literature, a dynamic simulation of the rolling process is carried out, and the stress, strain and temperature field of the axle steel in the forming process are analysed. The results show that with the deepening of rolling, the plastic deformation of the metal becomes increasingly obvious. When the finishing section is reached, the temperature on the surface and inside the rolled piece reaches relatively uniform distribution.

Key words: *cross-wedge rolling, LZ50 axle steel, finite element model, dynamic simulation, forming analysis*

1. Introduction

Cross-wedge rolling (CWR) is a forging process in which the upper and lower rolls rotate to drive the rolling stock to rotate and form, and it is also an advanced manufacturing technology [1-4]. Its working principle is to install and fix two wedge-shaped dies on the two parallel rolls up and down, so that they rotate in the same direction, and use the friction force between the roll and the rolling piece to drive the rolling piece to rotate in the opposite direction. Through the action of the mould, a variety of shaft parts are formed.

Experts and scholars have carried out many studies on the rolling technology of cross-wedge rolling [5-7]. Significant results have been achieved in cross-wedge rolling damage simulation, cross-wedge rolling forming research, cross-wedge rolling for large axles, three-roll cross-wedge rolling technology, and important process parameters for cross-wedge rolling.

(1) Injury simulation of cross-wedge rolling

Tianxiang Li et al. [8] selected crack-sensitive steel EH47 with the microalloying element Nb as research material and used the finite element model (FEM) analysis method to predict surface ductile fracture in the process of HHR2. Zbigniew Pater et al. [9] studied the prediction of material cracks in cross-wedge rolling, analysed 54 cases of damage by using the finite element method, and determined the maximum value of the damage function. M.F. Novella et

al. [10] revised the Oyane-Sato fracture criterion, proposed a correlation between temperature and the strain rate, and applied it to the high-temperature cross-wedge rolling process of AA6082-T6 bars. A comparison of numerical and experimental results verifies the validity of the fracture criterion.

(2) Cross-wedge rolling for large axles

Xuelei Zeng [11] took the hollow axle as a research object, and used theoretical analysis, numerical simulation and other research methods to study the die design and microstructure evolution of the multi-wedge rolling hollow axle. Xu Huang [12] carried out a rolling experiment of reducing the ratio of the variable inner diameter of the automobile hollow shaft head, laying the foundation for the efficient and economical production of the variable inner diameter hollow parts by cross-wedge rolling. Zhigang Li [13] developed a new set of cross-wedge rolling equipment to roll train axles.

(3) Three-roll cross-wedge rolling technology

Based on an analysis of the rolling principle of cross-wedge rolling, Jiangjiang Xu [14] focused on three-roll cross-wedge rolling technology and developed a symmetrical rolling method for asymmetrical parts with slender special-shaped section stepped shafts. Weidong Liu [15] used the radial strain gradient method to describe the process of loose formation and concluded that the cyclic tensile and compressive stress and strain is an important reason for the looseness of the core of three-roll cross-wedge rolling. Zhanjiang Jia [16] used two methods of three-roll cross-wedge rolling and hot rolling to study the forming principle of a tapered slender shaft.

(4) Important process parameters of cross-wedge rolling

Xinyan Zhang et al. [17] analysed the influence of three structural parameters of roller blade baffle clearance, base circle diameter, and widening angle on the forming quality of the tapered end in the process of roll cutting. Tomasz Bulza et al. [18] controlled the rolling process from three aspects of energy consumption, load and tool abrasive wear, and analysed the stress and strain during the rolling process at different temperatures. Cuiping Yang et al. [19] studied the influence of process parameters on the damage of the workpiece centre through an analysis of the stress-strain characteristics of the workpiece centre. Based on the results obtained from the simulation, Zbigniew Pater et al. [20] created a nomogram, and based on the basic CWR parameters (mainly forming angle, widening angle, and deformation ratio), the maximum damage function value can be quickly and easily determined.

To sum up, by establishing the geometric model of the cross-wedge rolling of axle steel and importing it into finite element simulation software for the dynamic simulation of the forming and analysis of stress, strain and temperature fields, it is possible to more accurately predict the forming process of the material. The rheological stress of the metal changes during the process. At the same time, it can also provide a theoretical basis and reference value for subsequent crack damage research and secondary development and application.

2. Model establishment

2.1 Establishment of the geometric model

This study uses LZ50 axle steel as the research object. As one of the widely used axle materials in China's railway manufacturing industry, LZ50 axle steel has sufficient strength and toughness [21-23]. When a high-speed rail runs at high speed, it can withstand multiple complex stresses such as rotational bending and shock vibration [24-26]. Therefore, compared with other types of axle steel, LZ50 steel has greater value based on research when choosing cross-wedge rolling for axle forming.

The part drawing of LZ50 axle steel is made by Solid works modelling software. The length of the axle steel is 100 mm and the diameter is 25 mm, as shown in **Fig. 1** below. To take into account the later deformation process, it is necessary to leave enough machining allowance for the axle blank, so, when designing and modelling, 5 mm is added at both ends of the rolled piece. Parts such as rolls, wedge-shaped moulds and baffles are drawn in turn, and finally assembled by modelling and assembly to form a set of overall assembly drawings, as shown in **Fig. 2**. Through the established assembly, it can be directly imported into the finite element analysis software through format conversion in the later stage for numerical simulation.

Fig. 1 Schematic diagram of the LZ50 axle steel

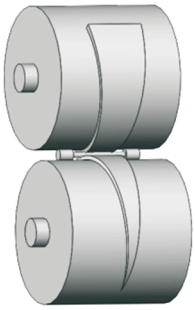

Fig. 2 Overall assembly diagram

2.2 Determination of rolling parameters

In the basic principles of die design for cross-wedge rolling, it is necessary to design appropriate die process parameters for better rolling. The following will discuss these process parameters in turn.

(1) Section shrinkage rate

The rate of reduction in the area is a basic process parameter in the design of the cross-wedge rolling die. The value of the reduction of area is the difference between the area after rolling and the area before rolling, and the ratio of the area before rolling. The calculation formula is:

$$\psi = \frac{F_0 - F_1}{F_0} = \frac{d_0^2 - d_1^2}{d_0^2} = 1 - \left(\frac{d_1}{d_0} \right)^2 , \tag{1}$$

where F_0 and d_0 are the area and diameter of the rolled piece before cross-wedge rolling, and F_1 and d_1 are the area and diameter of the rolled piece after cross-wedge rolling.

Under normal circumstances, the reduction rate of cross-wedge rolling should not be greater than 75%, otherwise it is easy to cause the phenomenon of non-rotation, necking, and breaking of the rolled piece during the forming process. At the same time, the area shrinkage rate should not be less than 35%. This is because when the area shrinkage rate is small, only the surface of the rolled piece will undergo plastic deformation under the compression of the roll during the rolling process, and the rolling forming will be incomplete. The centre of the rolled piece is loose.

To sum up, adopting an appropriate reduction of area can avoid secondary rolling and improve the forming quality of the rolled piece. Therefore, for cross-wedge rolling, the most favourable value for the reduction of the area is 50%-65%.

(2) Forming angle

The forming angle is the angle between the wedge slope and the bottom surface and is one of the two more important key process parameters in the design of the cross-wedge rolling

die. The selection of the appropriate forming angle has a great effect on the forming conditions of the rolled piece.

Under normal conditions, when a smaller forming angle is selected, the centre of the rolling stock will be loose or even fractured during the rolling process; when a larger forming angle is selected, the rotation conditions of the rolling stock will deteriorate rapidly. The risk easily arises of necking, but a larger forming angle can avoid the occurrence of central porosity. Therefore, choosing a moderate forming angle has a very profound impact on cross-wedge rolling.

In general, the value range of the forming angle is $18° \le \alpha \le 34°$.

Considering the value range of the forming angle, combined with the value relationship between the section shrinkage rate and the forming angle, **Table 1** summarizes the value relationship between the two:

Table 1 Relationship between the section shrinkage rate and the forming angle

Rate of reduction in area ψ /%	80～70	70～60	60～50	>50
Forming angle α /(°)	18～24	22～30	26～32	<28

(3) Widening angle

The widening angle, like the forming angle, is the other of the two more important key parameters in the design of the cross-wedge rolling die, and its selection plays a crucial role in ensuring the stability of the entire rolling process. In general, in order to reduce the length of the cross-wedge rolling die as soon as possible (the larger the length of the cross-wedge rolling die, the more difficult it is to design, instal and maintain the die), a larger widening angle is usually selected when designing the die.

According to the theoretical and practical basis, the selection range of the widening angle under most conditions is $4° \le \beta \le 12°$.

However, the effect of section shrinkage on the widening angle is special. When it is greater than 70%, selecting a larger widening angle will easily cause necking of the tie, so the value of the widening angle should be small; when it is less than 35%, selecting a larger widening angle is likely to cause central porosity in the rolled piece, so a smaller widening angle should also be selected at this time. **Table 2** lists the relationship between the reduction of area and the widening angle rolling stock:

Table 2 Relationship between the section shrinkage rate and the widening angle

Rate of reduction in the area ψ /%	80～70	70～60	60～50	50～40	<40
Widening angle β /(°)	4～8	5～9	7～12	5～9	<8

2.3 Rigid-plastic finite element method

The process of cross-wedge rolling the axle belongs to the hot working category in the volume forming stage, and the amount of elastic deformation is small during the forming process. Therefore, the rigid-plastic finite method can be used to analyse its forming process, which is equivalent to treating the axle material as rigid-plastic material for numerical processing [27-28]. Among them, some necessary assumptions need to be made before the material is processed, so that the deformation is idealized. Therefore, when using the rigid-plastic finite element method to analyse the deformation of metal materials, the material needs to meet the following assumptions:

(I) the homogeneous isotropy of metal materials;
(II) the elastic deformation of metal materials is ignored;
(III) the deformation flow of metal materials adopts the Levy-Mises rate equation and the Mises yield criterion;
(IV) the principle of the constant volume of metal materials;
(V) the work hardening of the material is not considered, and the sensitivity of the deformation resistance to the deformation speed is ignored.

Provided that the above assumptions are satisfied, the forming process of metal materials can be regarded as the forming process of rigid plastic materials. The following is an introduction to the basic principles of the rigid-plastic finite element method.

(1) Basic equation

Suppose the volume of the deformable body is V, the surface area is S, the given velocity V_i^o on a part of the velocity plane S_v of S, and a given surface force q_i on another part of the force surface S_t of S, then the basic equation satisfied by the metal material during the flow process is as follows:

① force balance equation

$$\sigma_{ij,j} + p_i = 0 \tag{2}$$

② force boundary conditions (on S_t)

$$\sigma_{ij} n_j = q_i \tag{3}$$

③ geometric equation

$$\dot{\varepsilon}_{ij} = \frac{1}{2}\left(v_{i,j} + v_{j,i}\right) \tag{4}$$

④ speed boundary condition (on S_v)

$$v_i = v_i^0 \tag{5}$$

⑤ volume incompressible equation

$$\dot{\varepsilon} = \delta_{ij}\dot{\varepsilon}_{ij} = 0 \tag{6}$$

⑥ yield criterion.

Using the *Mises* yield criterion and the isotropic hardening model, the initial yield criterion is:

$$\bar{\sigma} - \sigma_s = 0. \tag{7}$$

Subsequent yield conditions, considering only strain hardening for static loading, are:

$$\bar{\sigma} - K = 0, K = H\left(\int \mathrm{d}\bar{\varepsilon}\right). \tag{8}$$

In the formula, H can be determined from the uniaxial tensile test curve.

For rigid-plastic materials, the instantaneous yield condition is:

$$\bar{\sigma} - Y = 0, Y = Y\left(\varepsilon, \dot{\varepsilon}\right) \tag{9}$$

(2) Variational principle

In the above basic equations, although the variables of plastic deformation of metal materials can be obtained theoretically, in practice the practical problems need to be simplified before they can be solved by the traditional analytical methods above. Therefore, it is necessary to apply new finite element principles to solve the basic equations.

In the rigid-plastic finite element method, the deformed body is numerically analysed by using the *Markov* variational principle. The fully generalized variational principle is to find the extreme value of the energy functional, so that the real solution of the problem can be solved:

$$\Pi = \int_v E\left(\dot{\bar{\varepsilon}}\right)\mathrm{d}v - \int_{s_t} q_i v_i \mathrm{d}s \,. \tag{10}$$

The incomplete generalized variational principle is to construct a new functional on the basis of the original variational principle and perform a variational solution to this new functional. There are two main methods for this process: the Lagrange multiplier method and the penalty function method.

① Lagrange multiplier method

The Lagrange multiplier method is to introduce a Lagrange multiplier λ into the original functional to obtain a new functional, and then perform a variational solution to the new functional. The advantage of this method is that it has better convergence. However, new unknowns are introduced, which increases the difficulty of solving. The specific expression is as follows:

$$\Pi = \int_v E\left(\dot{\bar{\varepsilon}}\right)\mathrm{d}v - \int_{s_t} q_i v_i \mathrm{d}s + \int_v \lambda \dot{\varepsilon}_v \mathrm{d}v \,. \tag{11}$$

② Penalty function method

The penalty function method is to add a sufficiently large positive number α as a penalty factor to the volume incompressibility condition, and introduce it into the original functional as a penalty term to obtain a new functional:

$$\Pi = \int_v E\left(\dot{\bar{\varepsilon}}\right)\mathrm{d}v - \int_{s_t} q_i v_i \mathrm{d}s + \frac{a}{2}\int_v \left(\dot{\varepsilon}_v\right)^2 \mathrm{d}v \,. \tag{12}$$

During the solution process, when the velocity field is infinitely close to the real solution, the volume strain rate is close to 0, and the penalty term is also close to 0. The advantage of the penalty function is that the matrix has fewer dimensions, and the convergence is fast, but, at the same time, in the penalty function, its penalty factor cannot be taken too large, otherwise it will lead to an ill-conditioned equation system.

(3) Principle of virtual work

The virtual work principle is a general term for the virtual displacement (power) principle and the virtual stress (rate) principle. The virtual displacement (power) principle is the equivalent integral weak form of the equilibrium equation and the force boundary condition; the virtual stress (rate) principle is the geometric equation and the displacement boundary condition integral weak form. The virtual power equation is:

$$\int_v -\delta\dot{\varepsilon}_{ij}\sigma_{ij}\mathrm{d}v + \int_v \delta v_i p_i \mathrm{d}v + \int_{S_i} \delta v_i q_i \mathrm{d}s = 0 \,. \tag{13}$$

In the formula, the first term is the work done by the stress in the deformed body on the virtual strain rate, that is, the virtual power of the internal force; the second term is the virtual

power done by the body force; the third term is the virtual power done by the surface force. That is to say, the sum of the virtual power of the external force and the internal force is zero.

2.4 Establishment of the finite element model

Accordingly, the rigid-plastic finite element method is selected as the research method of this paper. In addition, when selecting the process die parameters, attention should be paid to the range of values to avoid unfavourable conditions such as necking and centre porosity during the forming process of the rolled piece [29-30]. **Table 3** shows the best forming parameters of the selected rolling stock and process die.

Table 3 Main process parameters of rolling parts and moulds

Name	Numeric value	Unit
Axle steel length	100	mm
Axle steel diameter	25	mm
The forming Angle	28	°
The width Angle	8	°
Reduction of area	60	%

According to the actual rolling condition of the cross-wedge rolling axle, the geometric model is converted into the format and imported into the ANSYS simulation software, as shown in **Fig. 3**. In the simulation process, the displacement constraints in the X, Y, and Z directions and the rotation constraints of the X and Y axes are respectively set for the roll, and the rotation speed of the roll around the Z axis is pre-set to 20r/min. In addition, the contact type between the roll and the rolling piece is selected as the shear friction type, and the rolling piece is divided into tetrahedron meshes; the number of meshes is about 20000, and the calculation step is 0.001s. The initial temperature of the roll was set at 20°C, and the initial temperature of the rolled product was set at 500°C.

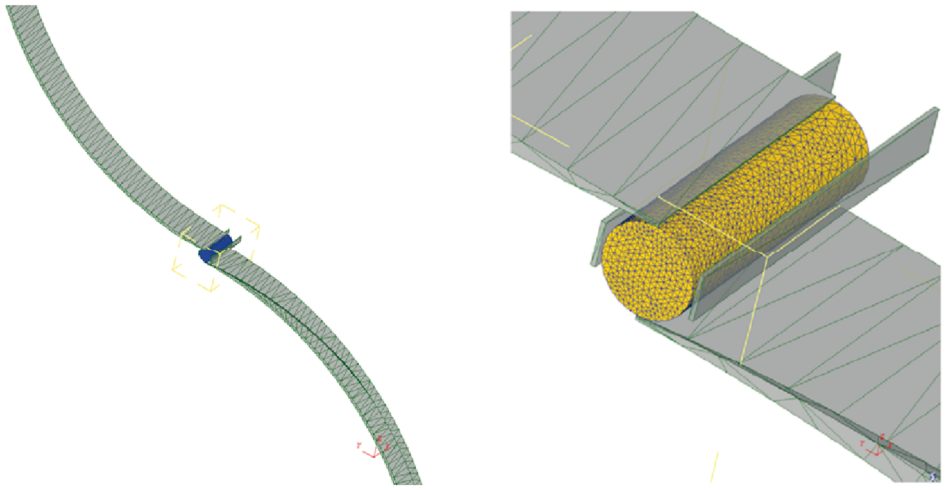

(a) Cross-wedge rolling model (b) Partially enlarged model

Fig. 3 Finite element model of cross-wedge rolling LZ50 axle

3. Simulation analysis of the forming process

3.1 Dynamic simulation of the forming of LZ50 axle steel

Because LZ50 axle steel is characterised as being difficult to form, before analysing the stress, strain and temperature field of the surface, the overall deformation process of the axle steel is firstly simulated dynamically, so that the overall deformation can be analysed. There is

a general understanding and mastery of the law of forming change. **Fig. 4** shows the strain distribution of the surface part of LZ50 axle steel at each moment, which can be divided into the following three parts according to the different stages of cross-wedge rolling for symmetrical axle parts.

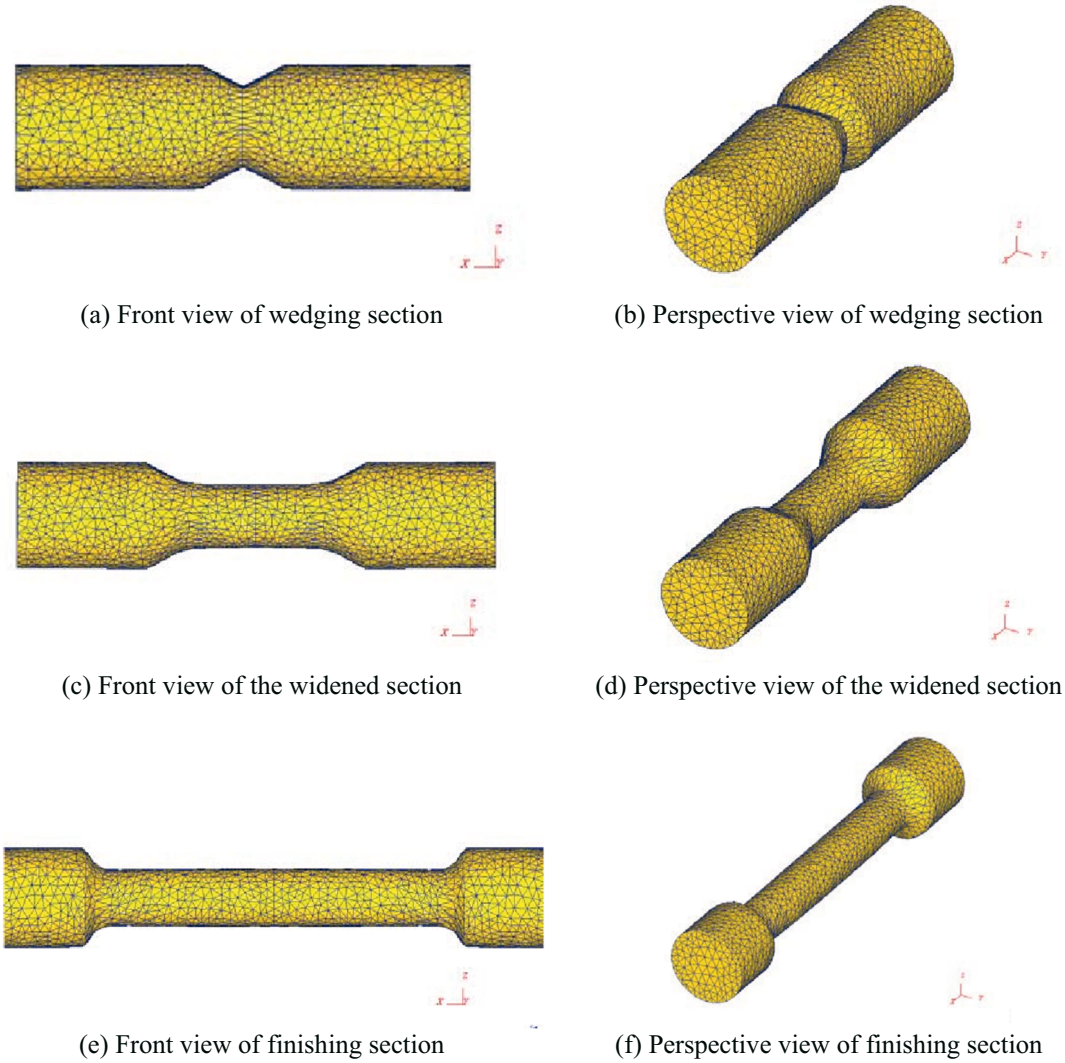

(a) Front view of wedging section
(b) Perspective view of wedging section
(c) Front view of the widened section
(d) Perspective view of the widened section
(e) Front view of finishing section
(f) Perspective view of finishing section

Fig. 4 Dynamic simulation of LZ50 axle steel at different stages

From the different stages of the movement of the cross-wedge rolling die, it can be seen that when the die just enters the wedging stage, the plastic deformation is mainly concentrated on the surface of the rolled piece, and the amount of strain at this time is small. With the deepening of the rolling, the plastic deformation on the surface of the rolling piece gradually penetrates into the core, and the amount of strain increases gradually. As the rolling continues, some of the *V*-grooves extruded on the rolling stock reach the minimum rolling radius and are partially widened. When all reach the minimum radius, the radius of the rolled piece does not change, but the width of the rolled piece is still changing at this time, which is normal expansion. When the finishing stage is reached, the radius and width of the rolling stock do not change, and the deformation work of the rolling stock ends.

3.2 Stress field analysis of the forming of LZ50 axle steel

Through the research and analysis of the dynamic simulation of the forming of LZ50 axle steel, the forming process of the cross-wedge rolling axle has generally been grasped. Therefore, in the stress field analysis of the forming process, the stress analysis is carried out

on the wedge section, the widening section and the finishing section respectively, so that the stress at each stage of the cross-wedge rolling during the rolling of the axle steel can be more accurately predicted.

3.2.1 Stress analysis of the longitudinal section of the wedge section

The stress field distribution of the longitudinal section of the wedge section during the forming of LZ50 axle steel is shown in **Fig. 5.** The three-direction stress (radial stress, axial stress and transverse stress) are simulated and analysed respectively. It can be seen from the stress distribution diagram that in the wedging section, the radial, axial and lateral parts of the rolling piece are mainly subjected to compressive stress from the wedge-shaped die of the roll, and larger pressure is generated on the surface in contact with the die. The maximum compressive stress value can reach -600 MPa; the compressive stress value in the part away from the contact area is gradually reduced until it drops to zero. The compressive stress at the core of the rolling stock is almost zero, because only a small amount of plastic deformation occurs at the contact surface between the rolling stock and the roll during the wedging section, and this part of the plastic deformation is not enough to extend to the rolling stock.

To sum up: compressive stress is mainly borne at the wedging section.

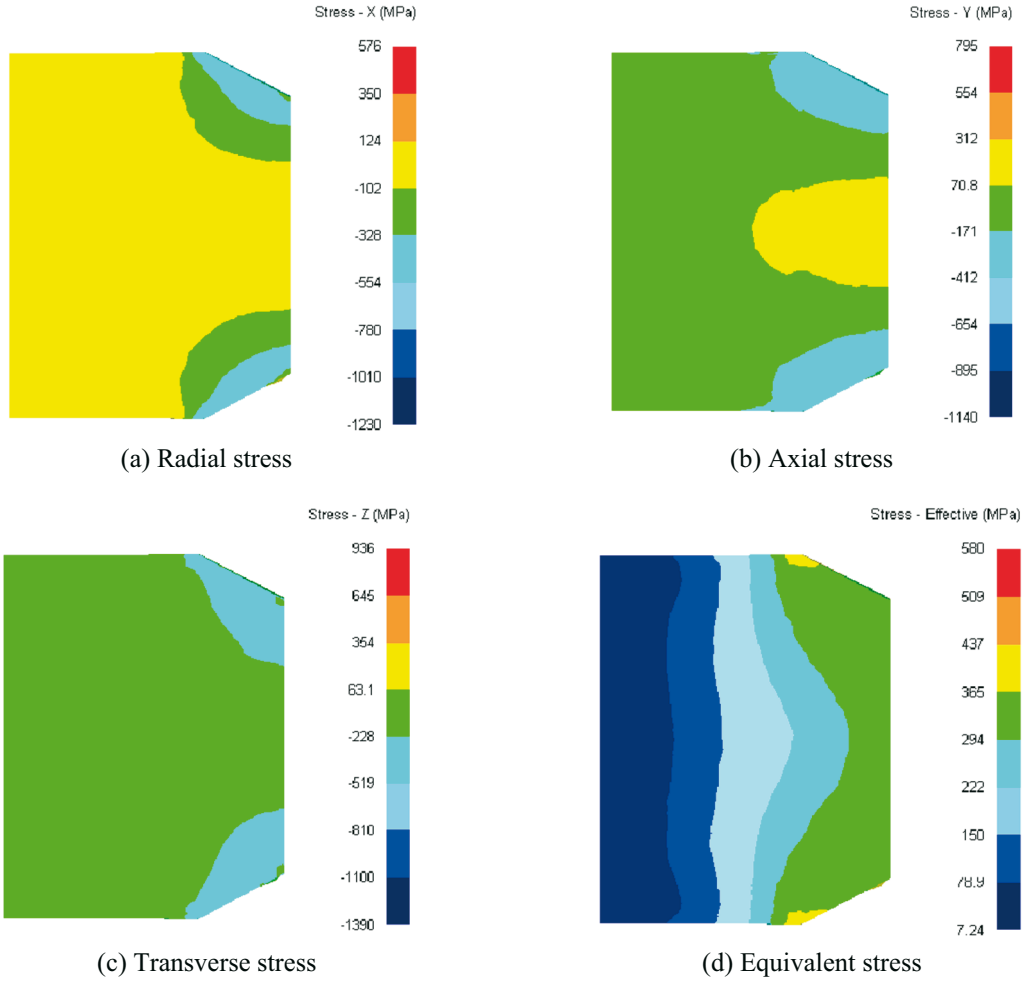

(a) Radial stress (b) Axial stress

(c) Transverse stress (d) Equivalent stress

Fig. 5 Vertical section stress field distribution of the wedge section

3.2.2 Stress analysis of the longitudinal section of the widened section

The stress field distribution of the longitudinal section of the widened section of LZ50 axle steel during forming is shown in **Fig. 6**. In the widening section, with the deepening of the

cross-wedge rolling, it can be seen from the distribution of radial stress (a) and axial stress (b) that there are both tensile stress and compression in the contact surface area between the roll and the workpiece. In the specific analysis, in the area A where the wedge is in contact with the rolling piece, the compressive stress is the main one, and the maximum compressive stress can reach -1200MPa, while the tensile stress is the main stress in other contact areas. It can be seen from the transverse stress (c) that the main stress of the rolling piece is mainly tensile stress, and the maximum tensile stress can reach 491 MPa.

To sum up: at the widening section, the rolling stock is subjected to both tensile and compressive stress. But in radial and axial stress, there is mainly compressive stress; in the transverse stress, there is mainly tensile stress.

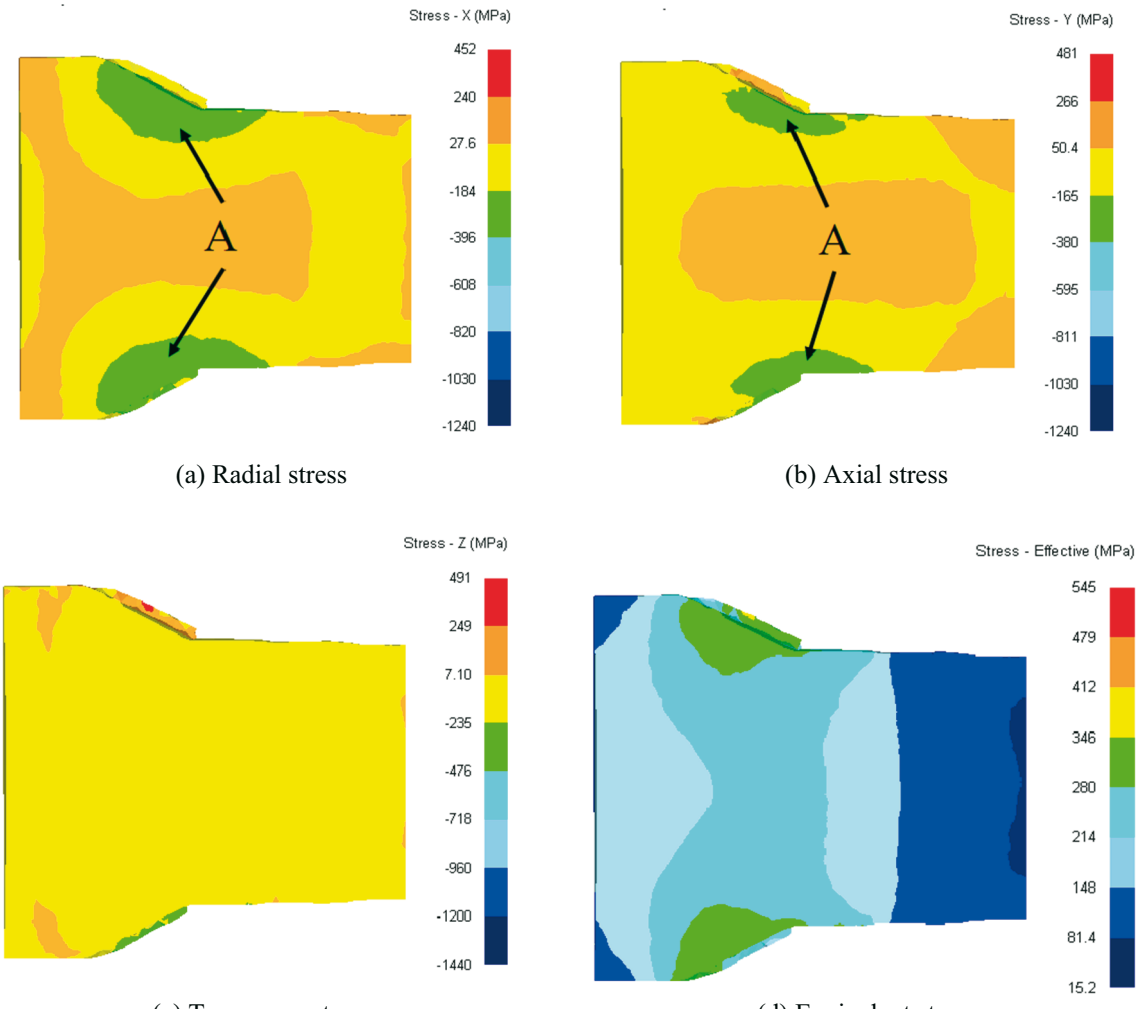

(a) Radial stress (b) Axial stress

(c) Transverse stress (d) Equivalent stress

Fig. 6 Distribution of the longitudinal section stress field in the widened section

3.2.3 Stress analysis of the finishing section of the longitudinal section

Fig. 7 shows the stress field distribution of the finishing section of LZ50 axle steel during forming. During the finishing section, in the contact area between the surface of the rolling piece and the wedge, the main generating area of compressive stress has a numerical range of -400 to -900 MPa in the radial, axial and transverse directions. From the axial stress (b) and transverse stress (c) diagrams, it can be clearly seen that in the centre of the rolling piece, there is a tensile stress area, and the maximum stress can reach +400MPa, which is due to the rolling process. Severe axial and transverse plastic deformation occurs in the rolling stock, so that the

rolling stock is stretched, and tensile stress also occurs in the core. In radial stress (a), radial compression of the rolled product occurs.

To sum up: in the finishing section, the rolling stock is subjected to both tensile and compressive stresses. But in the axial and transverse stress, tensile stress is the main one; in the radial stress, compressive stress is the main stress.

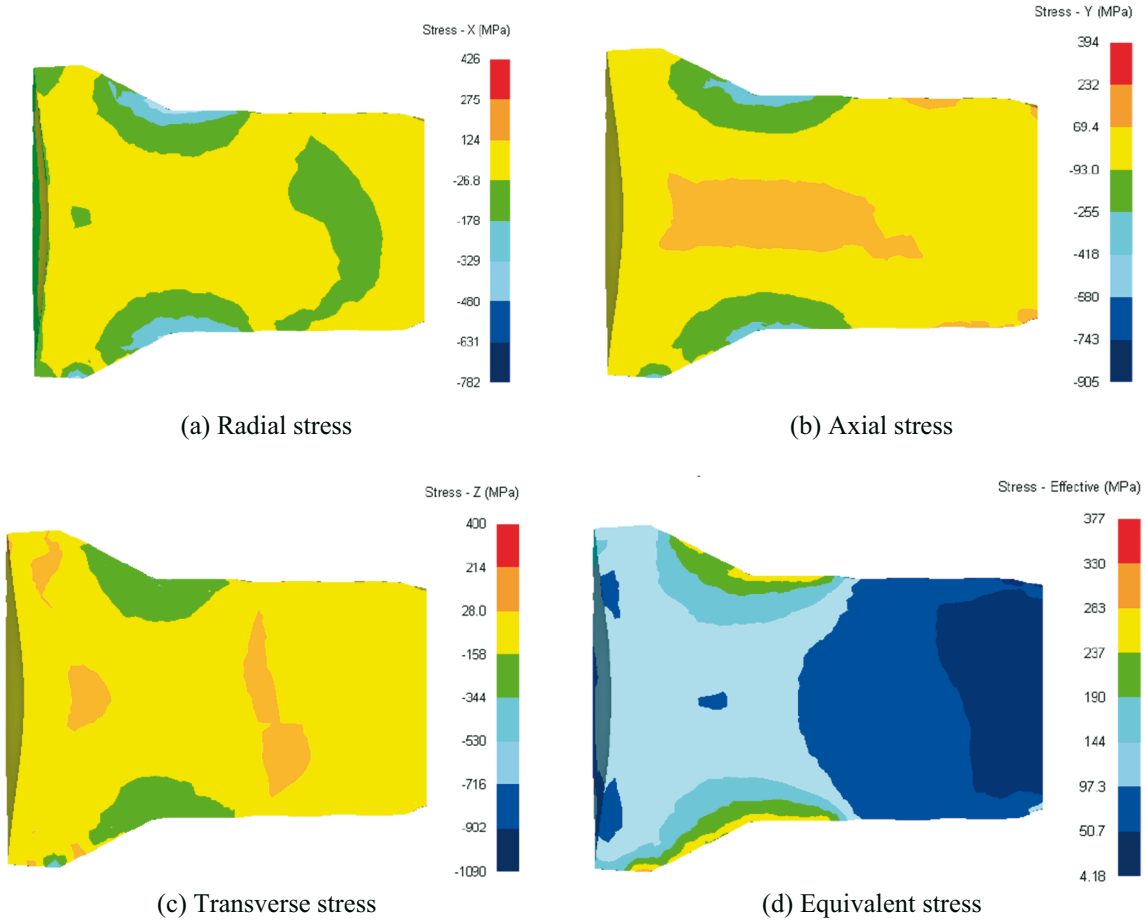

(a) Radial stress (b) Axial stress

(c) Transverse stress (d) Equivalent stress

Fig. 7 Vertical section stress field distribution in the finishing section

3.3 Strain field analysis of the forming of LZ50 axle steel

The strain field of LZ50 axle steel forming not only reflects the deformation of the rolling stock during the plastic forming process, but also shows the characteristics of metal flow during the deformation process. The deformation law plays a certain theoretical guiding role. This section presents a strain analysis of the cross-wedge rolling of axle steel in the wedging section, the widening section and the finishing section.

3.3.1 Strain analysis of the longitudinal section of the wedge section

Fig. 8 shows the strain field distribution of the longitudinal section of the wedge section of LZ50 axle steel during forming. During the wedging section, it can be seen from the radial strain diagram (a) that the tensile strain occurs in the contact area with the roll, and the maximum value is +0.718; the strain value gradually decreases to zero away from the contacted area. According to the axial strain diagram (b), it can be seen that compressive strain occurs at the wedging section A with a maximum value of -1.28, while tensile strain occurs at the rolled piece B with a maximum value of +0.714; this is because under the compressive action of the wedge-shaped die, the surface at A receives compressive strain along the axial direction, and

driven by the compressive strain at A, a small part of tensile strain will appear on the surface of the rolled piece. According to the transverse strain diagram (c), it can be seen that compressive strain occurs at the forming part of the rolled piece, and the maximum value is -1.36; when it is away from the contact area, the strain value gradually decreases. According to the equivalent strain diagram of the wedging section (d), it can be seen that the equivalent strain value of the surface of the rolling piece at the wedge is the largest, and the maximum value can reach 4.73. In the area far away from the contact between the rolling piece and the roll, the variable value of the equivalent effect variable gradually showed a decreasing trend.

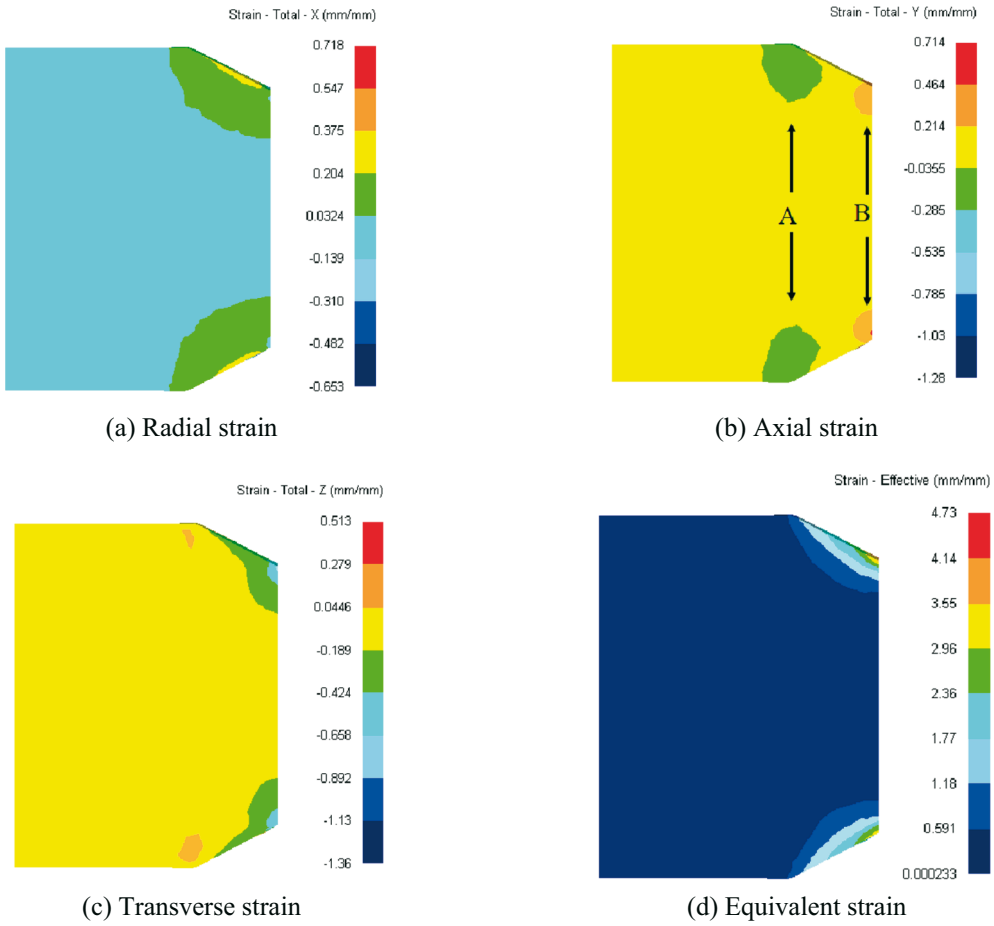

(a) Radial strain (b) Axial strain

(c) Transverse strain (d) Equivalent strain

Fig. 8 Vertical section strain field distribution of the wedge section

To sum up: at the wedge section, in the radial strain, tensile strain is mainly generated; in the axial strain, both tensile and compressive strain are generated; in the transverse strain, the compression is mainly generated strain.

3.3.2 Strain analysis of the longitudinal section of the widened section

Fig. 9 shows the strain field distribution of the longitudinal section of the widened section of LZ50 axle steel during forming. In the widening section, it can be seen from the radial strain diagram (a) that compressive strain occurs in the formed part of the rolled piece, and the maximum strain value is -1.37, and the strain value gradually increases from the forming area to the unformed area. According to the axial strain diagram (b), it can be seen that the tensile strain in the formed area of the rolled piece is the maximum value of +1.03, which appears in the core of the rolled piece. According to the transverse strain diagram (c), it can be observed that the strain distribution of the rolled piece is dominated by compressive strain in the forming area and tensile strain in the unformed area. According to the equivalent strain diagram of the

widening section (d), it can be noted that the overall strain intensity of plastic deformation gradually weakens from the forming area to the unformed area, and the deformation degree of the rolled piece is the largest in the forming area.

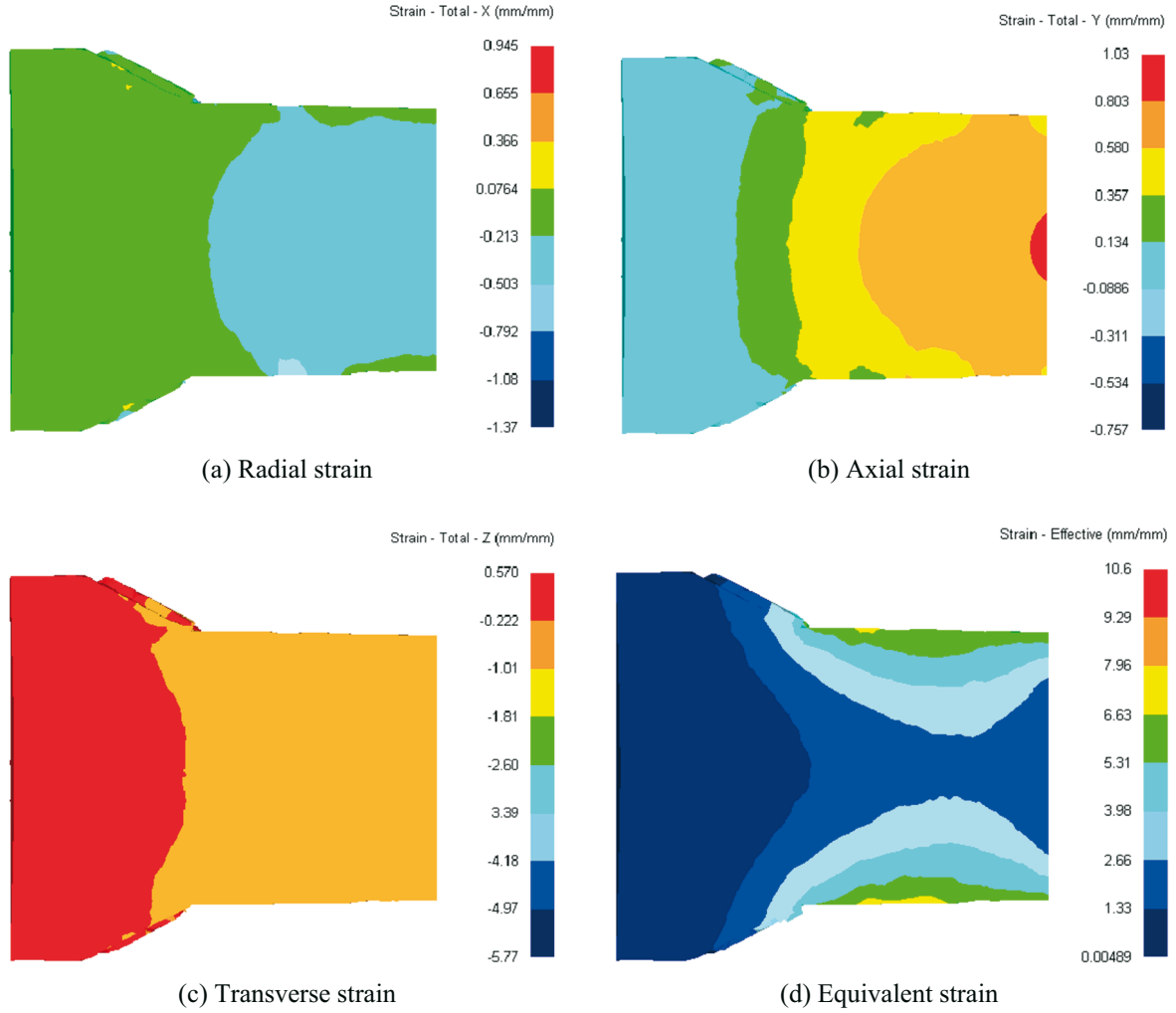

(a) Radial strain (b) Axial strain

(c) Transverse strain (d) Equivalent strain

Fig. 9 Distribution of the longitudinal strain field in the widened section

To sum up: at the widening section, in the radial strain, compressive strain is mainly produced; in the axial strain, tensile strain is mainly generated, especially in the core of the rolled piece. In the transverse strain, compressive strain occurs in the formed area and tensile strain occurs in the unformed area.

3.3.3 Strain analysis of the longitudinal section of the finishing section

Fig. 10 shows the strain field distribution of the finishing section of LZ50 axle steel during forming. During the finishing section, in radial strain (a), compressive strain is dominant in the formed area, with a maximum value of -1.01, and there is partial tensile strain in the unformed area of the shaft end. In axial strain (b), the thinned forming part is dominated by axial tensile strain, because at the finishing section the forming area of the rolled piece is squeezed by the wedge die. At the end of the rolled piece, compressive strain is dominant. In transverse strain (c), the transverse surface is dominated by compressive strain, while in the interior of the rolled piece it is dominated by tensile strain. According to the equivalent strain diagram of the widening section (d), it can be seen that during the finishing section, there is large plastic deformation, and there is great strain strength in the thinned part of the rolled piece, while in the area far from the thinner part, the strain strength gradually decreases.

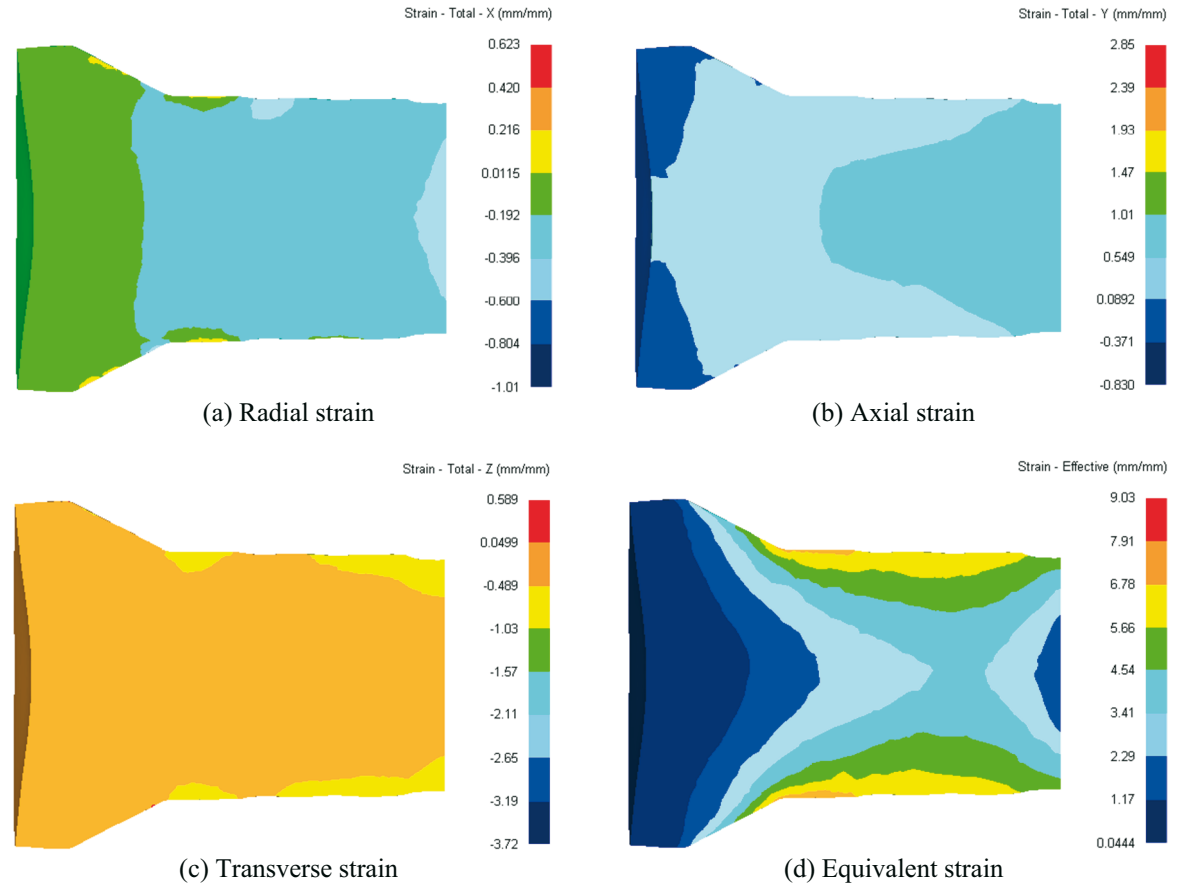

(a) Radial strain (b) Axial strain

(c) Transverse strain (d) Equivalent strain

Fig. 10 Vertical section strain field distribution in the finishing section

To sum up: in the finishing section, in radial strain and transverse strain, compressive strain is mainly produced, but some tensile strain is created at the end of the rolled piece; in axial strain, tensile strain is mainly generated.

3.4 Analysis of the temperature field distribution characteristics of the forming of LZ50 axle steel

LZ50 axle steel has good high-temperature resistance, and also has sufficient strength and toughness. However, if the forming temperature cannot be well grasped during the cross-wedge rolling process, it is easy to cause overheating and burning of the rolled piece. Therefore, it is very important to control the optimum rolling temperature during the forming process for the forming of the rolled product. This section simulates and analyses the temperature field changes in the wedging section, widening section and finishing section of cross-wedge rolling axle steel, and focuses on the temperature field changes in the longitudinal section and the surface of the rolled piece. Later research on the forming of LZ50 axle steel and the actual rolling process played an important role in laying the groundwork.

3.4.1 Analysis of the temperature field in the wedge section

As shown in **Fig. 11**, from the temperature field distribution (a) of the circular section of the wedge section, it can be seen that the temperature in the contact area on the surface of the rolling stock is significantly higher than that in the core of the rolling stock, and the temperature in the unformed area does not rise significantly. From the temperature field distribution (b) of the longitudinal section of the wedge section, it can be seen that in the wedge section, due to plastic deformation, the surface temperature of the contact surface between the wedge die and the rolling piece gradually increases, and the maximum temperature can reach 1120 °C; the temperature of the untouched area did not change. This is because during the wedging period,

only a small part of the plastic deformation occurs on the surface of the rolled piece, and this part of the plastic deformation is converted into heat energy. Since the thermal conductivity of axle steel is relatively poor, the heat energy cannot be significantly transferred.

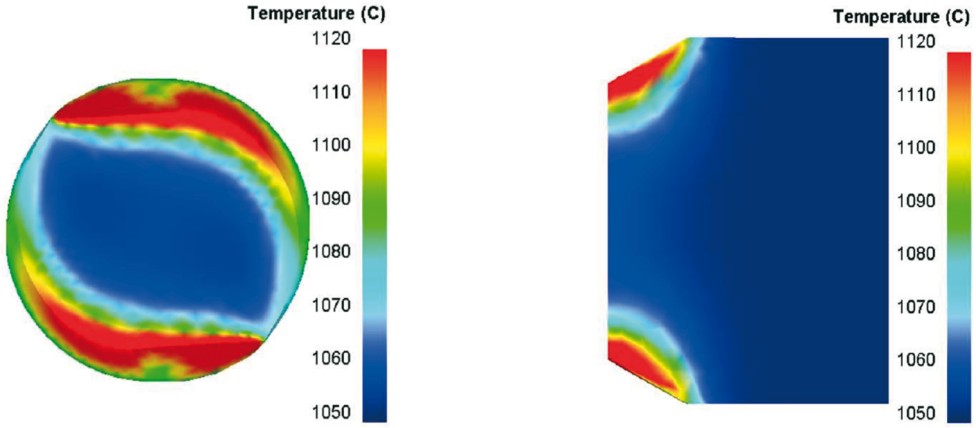

(a) Temperature field distribution of the circular section (b) Temperature field distribution of the longitudinal section

Fig. 11 Wedge section of the LZ50 axle steel temperature field

To sum up, in the wedging period, only part of the plastic deformation occurs during the forming process; the temperature of the forming area of LZ50 axle steel is higher than that of the unformed area, and the surface temperature of the rolled piece is higher than the core temperature.

3.4.2 Analysis of the temperature field in the widening section

As shown in **Fig. 12**, it can be seen from the temperature field distribution (a) of the circular section of the widening section that the temperature gradually decreases from the surface area to the centre, and with the severe plastic deformation during the widening section, the plastic work is converted into heat energy. The distribution effect is also enlarged, so that the overall temperature of the rolling stock is increased. It can be seen from the temperature field distribution (b) of the longitudinal section of the widening section that in the widening section, with the deepening of the plastic deformation, the temperature at the contact between the wedge-shaped die and the rolling piece reaches the highest value, which is 1180 °C. The temperature variation is small, and the distribution law of the temperature field gradually decreases from the forming area to the unformed area.

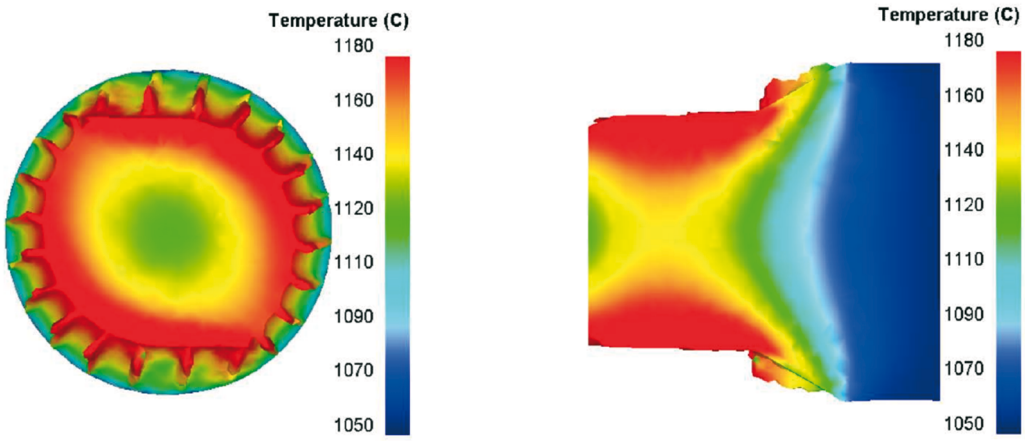

(a) Temperature field distribution of the circular section (b) Temperature field distribution of the longitudinal section

Fig. 12 Widened section of the LZ50 axle steel temperature field

To sum up: in the period of widening, large plastic deformation occurs, which makes the forming area temperature of LZ50 axle steel reach the highest point of 1180°C.

3.4.3 Analysis of the temperature field in the finishing section

As shown in **Fig. 13**, it can be seen from the temperature field distribution of the longitudinal section of the finishing section that in the finishing section the temperature in the contact area can reach 1220 °C, and the temperature in the core of the rolled piece can also reach 1200 °C. The temperature distribution gap between the contact area and the core of the piece gradually decreases. In addition, the end temperature of the rolling stock increases compared with the end temperature during the widening period, and the temperature difference in each area of the rolling stock surface is not great; this is because in the finishing period the forming change area becomes stable, and the change in temperature value reaches the maximum.

To sum up: in the finishing period, the plastic deformation gradually tends to be stable. At the same time, due to the poor thermal conductivity of LZ50 axle steel, it is difficult to dissipate heat to the outside, so the temperature distribution between the surface and the inside of the rolled piece is relatively uniform.

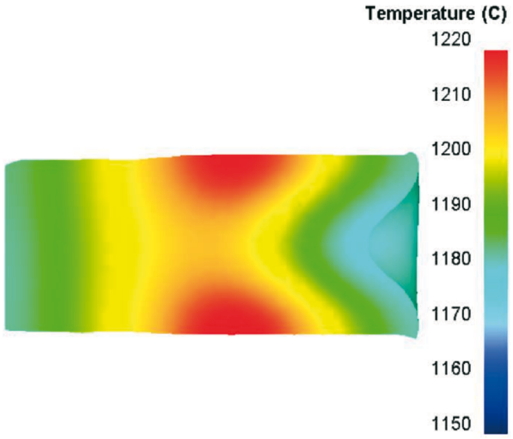

Fig. 13 Finishing section of the LZ50 axle steel temperature field

4. Conclusion

In this paper, through the rigid-plastic finite element analysis method, combined with reference literature and previous model application comprehensive research, ANSYS simulation software was selected to simulate and analyse the overall deformation, stress field, strain field and temperature field distribution of LZ50 axle steel. The main conclusions are as follows:

(1) In the dynamic simulation analysis of LZ50 axle steel, under the action of a wedge-shaped die, the rolling stock will have the characteristics of radial compression, lateral deformation and axial extension; among them, radial compression and axial extension should be the main deformation of the piece.

(2) In the process of stress field analysis, the rolling stock mainly bears compressive stress at the wedging section; at the widening section and finishing section, the rolling stock bears both tensile stress and compressive stress.

(3) In the process of strain field analysis, the rolling stock will produce tensile strain and compressive strain in each period, and the specific strain conditions should be determined according to the three-dimensional strain conditions of each stage.

(4) In the analysis of the temperature field, during the wedging period, due to the small plastic deformation, a higher temperature is generated only on the surface of the wedge; during the widening period, the rolling piece will undergo large plastic deformation, and the

temperature of the rolling piece surface will also reach the highest level at this time; during the finishing period, the plastic deformation gradually becomes stable, and the thermal conductivity of the axle steel is poor, so it is difficult to reduce the temperature. The surface and internal temperatures are uniform.

Declaration of Competing Interest

The authors declare that they have no known competing financial interests or personal relationships that could have appeared to influence the work reported in this paper.

Acknowledgements

This work is supported by projects funded by national key research and development plans of China (Grant No. 2018YFB1307902) and Shanxi Provincial Science and Technology Platform Project (Grant 201805D121006).

REFERENCES

[1] Yingxiang Xia, Xuedao Shu, Debiao Zhu et al. Effect of process parameters on microscopic uniformity of cross wedge rolling of GH4169 alloy shaft. Journal of Manufacturing Processes, **2021**,66: 145-152. https://doi.org/10.1016/j.jmapro.2021.03.063

[2] Lei Zhao. Research on micro-cross-wedge rolling forming process of Zr-based amorphous alloy micro-shafts. Yanshan University, **2021**.

[3] Zhixiang Chen. Research on the key technology of superalloy shaft cross wedge rolling. Ningbo University, **2020**.

[4] Ji Chen. Theoretical research on warm rolling forming process of cross wedge rolling shafts. Ningbo University, **2020**.

[5] Aleksandar Todić, Milan T. Djordjević, Dušan Arsić et al. Influence of vanadium content on the tribological behaviour of X140CrMo 12-1 air-hardening steel. Transactions of FAMENA, **2022**,46(2): 15-22. https://doi.org/10.21278/TOF.462035021

[6] Z. Pater. Finite element analysis of cross wedge rolling. Journal of Materials Processing Technology **2006**,173, 201-208. https://doi.org/10.1016/j.jmatprotec.2005.11.027

[7] Jiri Stodola, Petr Stodola. Analysis and model of corrosion of selected materials used in special vehicles. Transactions of FAMENA, **2021**, 45(4): 13-27. https://doi.org/10.21278/TOF.454022820

[8] Tianxiang Li, Haijun Li, Ruihao Li et al. Analysis of ductile fractures at the surface of continuous casting steel during. Journal of Materials Processing Tech., **2020**,283. https://doi.org/10.1016/j.jmatprotec.2020.116713

[9] Pater Zbigniew, Tomczak Janusz, Bulzak Tomasz et al. Determination of the critical damage for 100Cr6 steel under hot forming conditions. Engineering Failure Analysis, **2021**, 128. https://doi.org/10.1016/j.engfailanal.2021.105588

[10] Novella M.F., Ghiotti A., Bruschi S. et al. Ductile damage modeling at elevated temperature applied to the cross wedge rolling of AA6082-T6 bars. Journal of Materials Processing Tech., **2015**, 222: 259-267. https://doi.org/10.1016/j.jmatprotec.2015.01.030

[11] Xuelei Zeng. Study on the microstructure law of cross-wedge and multi-wedge synchronous rolling hollow axles. Ningbo University, **2012**.

[12] Xu Hang. Research on key technology of 40MnBH hollow shaft cross wedge rolling based on mandrel control. University of Science and Technology Beijing, **2019**.

[13] Zhigang Li. New equipment and new process for refined billet cross wedge rolling for train axles. Jilin University, **2010**.

[14] Jiangjiang Xu. Simultaneous rolling technology of three-high cross wedge rolling. Yanshan University, **2011**.

[15] Weidong Liu. Simulation research on forming mechanism of three-roll cross wedge rolling. Yanshan University, **2010**.

[16] Zhanjiang Jia. Design and simulation research on three-roll cross wedge rolling with tapered elongated shaft. Yanshan University, **2013**.

[17] Xinyan Zhang, Ying Wang, Pengke Hu et al. Design and experiment of roll-cut forming device for tapered end blanks. China Mechanical Engineering, **2021**, 32(17): 2100-2107.

[18] Bulzak Tomasz, Pater Zbigniew, Tomczak Janusz et al. Hot and warm cross-wedge rolling of ball pins: Comparative analysis. Journal of Manufacturing Processes, **2020**, 50: 90-101. https://doi.org/10.1016/j.jmapro.2019.12.001

[19] Cuiping Yang, Hongbiao Dong, Zhenghuan Hu. Micro-mechanism of central damage formation during cross wedge rolling. Journal of Materials Processing Tech., **2018**, 252: 322-332. https://doi.org/10.1016/j.jmatprotec.2017.09.041

[20] Pater Zbigniew, Tomczak Janusz, Bulzak Tomasz. Rapid estimation of ductile crack formation in cross-wedge rolling. Journal of Materials Research and Technology, **2020**, 9(6): 14360-14371. https://doi.org/10.1016/j.jmrt.2020.10.046

[21] Zhibiao Xu, Jinfang Peng, Jianhua Liu et al. Investigation of fretting fatigue behavior and micro-structure evolution in LZ50 steel subjected to torsional load. International Journal of Fatigue, **2019**, 128. https://doi.org/10.1016/j.ijfatigue.2019.06.033

[22] Zhibiao Xu, Jinfang Peng, Jianhua Liu et al. Study on fretting wear and tribo-chemical behavior of LZ50 axle steel in torsional fretting fatigue. Wear, **2019**, 426-427: 704-711. https://doi.org/10.1016/j.wear.2018.12.074

[23] Bing Yang, YongXiang Zhao. Experimental research on dominant effective short fatigue crack behavior for railway LZ50 axle steel. International Journal of Fatigue, **2012**, 35:71-78. https://doi.org/10.1016/j.ijfatigue.2010.11.012

[24] Maoyang Zhou, Pengtao Liu, Fengjiao Cao. Analysis of surface ultrasonic rolling modification of LZ50 axle steel. Equipment Management and Maintenance, **2021**(21): 26-30.

[25] Qian Liu, Xinyu Ning, Tianxiang Li et al. High-temperature viscoplastic constitutive model and rheological behavior analysis of axle steel. Journal of Northeastern University (Natural Science Edition), **2021**, 42(10): 1407-1413, 1426.

[26] Lianqing Wang, Yan Luo, Shengchuan Wu et al. Effect of shot peening on fatigue properties of axle steel damaged by foreign objects. Mechanical Design and Manufacture, **2021**(9):98-101, 106.

[27] Jingnan Liu, Changqing Ye, Guisen Liu et al. The finite element model of crystal plasticity in dynamic process of high temperature, high pressure and high strain rate and its application. Chinese Journal of High Pressure Physics, **2020**(34): No. 3.

[28] Na Li, Wensheng Yuan, Gang Cheng. Research on mechanical behavior and stiffness of cross wedge rolling mill body based on finite element theory. Forging Equipment and Manufacturing Technology, **2010**, 45(3): 52-55.

[29] Mohd Ahmed. Techniques for mesh independent displacement recovery in elastic finite element solutions. Transactions of FAMENA, **2021**, 45(2): 41-58. https://doi.org/10.21278/TOF.452019720

[30] Yuanming Huo, Qian Bai, Baoyu Wang et al. A new application of unified constitutive equations for cross wedge. Journal of Materials Processing Tech., **2015**, 223: 274-283. https://doi.org/10.1016/j.jmatprotec.2015.04.011

Submitted: 30.5.2022

Accepted: 31.8.2022

Hongwei Gao*
Qinhong Fan
Zhibing Chu
School of Mechanical Engineering,
Taiyuan University of Science and Technology, Taiyuan, Shanxi Province, China, 030024
*Corresponding author:
1059063799@qq.com